

1 **Timing of the first drainage of the Baltic Ice Lake synchronous**  
2 **with the onset of Greenland Stadial 1**

3 FRANCESCO MUSCHITIELLO, JAMES M. LEA, SARAH L. GREENWOOD, FAEZEH M. NICK,  
4 LARS BRUNNBERG, ALISON MACLEOD AND BARBARA WOHLFARTH

5 Muschitiello, F., Lea, J. M, Greenwood, S. L., Nick, F. M., Brunnberg, L., MacLeod, A., &  
6 Wohlfarth, B.: Timing of the first drainage of the Baltic Ice Lake synchronous with the  
7 onset of Greenland Stadial 1

8 Glacial varves can give significant insights into recession and melting rates of decaying  
9 ice sheets. Moreover, varve chronologies can provide an independent means of  
10 comparison to other annually resolved climatic archives, which ultimately help to  
11 assess the timing and response of an ice sheet to changes across rapid climate  
12 transitions. Here we report a composite 1257-year long varve chronology from south-  
13 eastern Sweden spanning the regional late Allerød-late Younger Dryas pollen zone.  
14 The chronology was correlated to the Greenland Ice Core Chronology 2005 using the  
15 time-synchronous Vedde Ash volcanic marker, which can be found in both  
16 successions. For the first time, this enables secure placement of the Lateglacial  
17 Swedish varve chronology in absolute time. Geochemical analysis from new varve  
18 successions indicate a marked change in sedimentation regime accompanied by an  
19 interruption of ice-rafted debris deposition synchronous with the onset of Greenland  
20 Stadial 1 (GS-1; 12 846 years before 1950 AD). With the support of a simple ice  
21 flow/calving model, we suggest that slowdown of sediment transfer can be explained  
22 by ice-sheet margin stabilisation/advance in response to a significant drop of the Baltic  
23 Ice Lake level. A reassessment of chronological evidence from central-western and  
24 southern Sweden further supports the hypothesis of synchronicity between the first  
25 (penultimate) catastrophic drainage of the Baltic Ice Lake and the start of GS-1 in  
26 Greenland ice cores. Our results may therefore provide the first chronologically robust  
27 evidence linking continental meltwater forcing to rapid atmosphere-ocean circulation  
28 changes in the North Atlantic.

29 *Francesco Muschitiello (Francesco.muschitiello@geo.su.se), Sarah L. Greenwood and*  
30 *Barbara Wohlfarth, Department of Geological Sciences and Bolin Centre for Climate*

31 *Research, Stockholm University, SE-10691, Stockholm, Sweden; James M. Lea and Lars*  
32 *Brunnberg, Department of Physical Geography and Bolin Centre for Climate Research,*  
33 *Stockholm University, SE-10691, Stockholm, Sweden; Faezeh M. Nick, Department of*  
34 *Geology, University Centre in Svalbard (UNIS), PO Box 156, NO-9171 Longyearbyen,*  
35 *Norway, Centre for Ice and Climate, Niels Bohr Institute, University of Copenhagen,*  
36 *2100 Copenhagen, Denmark; Alison MacLeod, Department of Geography, Royal*  
37 *Holloway University of London, Egham, Surrey TW20 0EX, UK.*

38 Understanding the timing and interplay between past ice-sheet dynamics and abrupt  
39 climate change can be significantly enhanced where suitable highly resolved and  
40 independently dated palaeoenvironmental archives are available. Glacial varves are  
41 such a proxy, providing an indirect record for ice-marginal dynamics at potentially  
42 annual or sub-annual resolution. Furthermore, these records can provide lengthy and  
43 continuous chronologies, which can be directly compared to other climate archives.  
44 In turn, this allows the examination of potential couplings between changing regional  
45 ice-sheet behaviour and climate change.

46         The Swedish glacial varve chronology or 'Swedish Time Scale' (STS) provides a  
47 reconstruction preserving information regarding the dynamics and the melting of the  
48 Fennoscandian Ice Sheet (FIS). It is therefore an ideal data set to investigate ice sheet  
49 dynamics and sensitivity in response to climate change. The STS is based on visual  
50 cross-correlation of more than 1000 ice-proximal clastic varve-thickness successions,  
51 which reflect the seasonal sediment input associated with the deglaciation of Sweden  
52 (De Geer 1912, 1940). These clastic varves, with their distinct silt dominated summer  
53 and clay dominated winter layers were deposited in the ice-dammed Baltic basin, the

54 Baltic Ice Lake (BIL), and can today be found along the Baltic Sea coast and in the Baltic  
55 Sea (Strömberg 1985; Cato 1987; Björck *et al.* 1992; Brunnberg 1995; Wohlfarth *et al.*  
56 1994, 1995). The younger part of the STS is made up of postglacial delta sediments,  
57 which were and still are deposited in the estuary of River Ångermanälven in northern  
58 Sweden (Cato 1985, 1987, 1998; Wohlfarth *et al.* 1997). However, a putative gap of  
59 700-900 varve years during the early and/or mid Holocene (Wohlfarth 1996;  
60 Wohlfarth *et al.* 1997; Andrén *et al.* 1999), as well as difficulties in correlating varve  
61 diagrams from Blekinge in southernmost Sweden to those of south-eastern Sweden  
62 (Wohlfarth & Possnert 2000) has so far posed a challenge to establishing an absolute  
63 and continuous varve chronology from present back to >14 000 varve years. Given  
64 the chronological uncertainties due to missing varves, each regional varve chronology  
65 thus stands on its own (Wohlfarth & Possnert, 2000).

66 The Lateglacial clay-varve diagrams from south-eastern Sweden (northern  
67 Småland and Östergötland) (Kristiansson 1986; Brunnberg 1995; Wohlfarth *et al.*  
68 1993, 1994, 1995, 1998), spanning the later part of the regional Allerød pollen zone  
69 (AL) and the early part of the regional Younger Dryas pollen zone (YD), constitute one  
70 of the most valuable portions of the STS. This Lateglacial varve chronology (LGC) is  
71 built by visual cross-correlations and corroborated by statistical analysis (Holmquist &  
72 Wohlfarth 1998), but is at present only tentatively linked to a calendar-year time scale  
73 by means of <sup>14</sup>C dating (Goslar *et al.* 1999; Wohlfarth & Possnert, 2000).

74 The recent finding of the Vedde Ash in a glacial varve succession from the same  
75 region (MacLeod *et al.* 2014) now offers an excellent opportunity to secure the  
76 floating LGC chronology to an absolute time scale, and more importantly, to correlate  
77 this section of the STS to the Greenland ice-core chronology. Through the temporal

78 accuracy this affords, the resulting correlation can therefore reveal crucial information  
79 regarding the temporal coupling between Fennoscandian ice-sheet dynamics and  
80 rapid climate change.

81 Here we reassess, update and extend the 806-year long LGC from south-eastern  
82 Sweden (Wohlfarth *et al.* 1998), and link for the first time the FIS recession to the  
83 Greenland ice-core time scale. The existing chronology has, moreover, been  
84 complemented by new geochemical data and corroborated by idealised numerical  
85 modelling of ice dynamics. These help to cast light on the changes that occurred in the  
86 BIL terminating sector of the FIS around the onset of the YD. Our results highlight a  
87 possible linkage between changes in ice sheet behaviour associated with the drainage  
88 of the BIL and abrupt changes in atmosphere-ocean circulation in the North Atlantic  
89 domain.

90

## 91 **Study area and methods**

### 92 *Study area*

93 The LGC derives from sites located along the eastern edge of the southern Swedish  
94 Uplands. The terrain reaches >330 m elevation above present-day sea level in the  
95 south and west of our area of interest, sloping eastwards and northwards towards the  
96 Baltic Sea (Fig. 1B, C). The FIS retreated broadly NW-wards across this region. Clay-  
97 varve chronologies have hitherto been the primary source of information regarding  
98 the pattern and timing of ice retreat (cf. Lundqvist & Wohlfarth 2001). An absence of  
99 moraines across south-eastern Sweden suggests unpunctuated retreat, an exception  
100 being the Vimmerby moraine that cuts across the south of our study area (Fig. 1C).  
101 Fed by fairly uniform SE-ward flow, this ice-margin position has been constrained by

102 cosmogenic nuclide dating to 14 600-14 400 cal. years ago (Johnsen *et al.* 2009; Anjar  
103 *et al.* 2014). There is no further evidence of a sustained ice-margin position until the  
104 Middle Swedish End Moraine Zone (MSEMZ), a broad (~10-20 km) zone stretching  
105 from Lake Vättern ENE across the Östergötland lowlands. Associated with the YD, the  
106 MSEMZ comprises moraines, deltas and glacio-tectonised successions linked with ice  
107 margin oscillations and an extremely slow rate of retreat (Kristiansson 1986; Lundqvist  
108 1987).

109         Glacial lakes were impounded across south-eastern Sweden in front of the  
110 retreating ice margin, both localised and linked to the much larger BIL, which was up-  
111 dammed in the Baltic Sea Basin. The BIL was maintained by the ice dam across central-  
112 southern Sweden and the southern Swedish uplands and the high threshold level in  
113 Öresund; not until the ice margin retreated past Mt. Billingen could any drainage occur  
114 (Björck 1995). A major (25 m lake-level drop) and rapid (1-2 years) drainage of the BIL,  
115 and consequent opening to marine waters (Yoldia Sea stage), occurred at the end of  
116 the YD when the Billingen ice dam was released (Björck & Digerfeldt 1984; Björck  
117 1995; Johnson *et al.* 2013). An earlier drainage is hypothesised to have occurred at the  
118 late AL-YD transition (Björck 1995; Bennike & Jensen 2013), but its magnitude and  
119 dynamics are less well-constrained. Palaeo-shorelines of the BIL are evident along the  
120 east and south coast of Sweden, rising to the north as a consequence of post-glacial  
121 (and ongoing) glacio-isostatic rebound (see Fig. 1).

122         AL-age glacial varved-clay successions from sites close to the former highest  
123 shoreline of the BIL had earlier been investigated in the provinces of Småland and  
124 Östergötland (Kristiansson 1986; Wohlfarth *et al.* 1995, 1998) (Fig. 1). Most of the  
125 varve thickness diagrams were obtained in a region that formed an archipelago-like

126 landscape in the western part of the large BIL (Wohlfarth *et al.* 1998). The glacial  
127 varves were thus deposited in fairly shallow waters (between ~5 and 70 m) and mostly  
128 within a large fjord complex (Fig. 1). Owing to isostatic uplift of the newly deglaciated  
129 areas, progressive shallowing of the depositional basins along the coast and successive  
130 isolation resulted in a cessation of varve deposition and replacement by homogeneous  
131 clay and organic lacustrine sediments. The recently published varve chronology from  
132 Gropviken (MacLeod *et al.* 2014) and the varve chronology from Sandfjärden (this  
133 study), ~50 km farther to the east, derive from sites that were located directly south  
134 of the YD ice margin (Fig. 1) and at a former BIL water depth of approximately 100 m  
135 (Brunnberg 1995).

136

### 137 *Varve and <sup>14</sup>C chronologies*

138 The original master chronology for Småland/Östergötland (the LGC) is a composite  
139 chronology of 806 varve years (Wohlfarth *et al.* 1998; Wohlfarth & Possnert 2000),  
140 which is based on the visual linking of common and distinct sedimentological features  
141 in 55 varve diagrams (Figs. 1, 2). These correlations are corroborated by cross-  
142 correlation analysis (Holmquist & Wohlfarth 1998). The chronology from Gropviken is  
143 a 710 varve-year long record, which contains the Vedde Ash isochrone (MacLeod *et*  
144 *al.* 2014). The chronology from Sandfjärden is a 623 varve-year long record (Fig. 1C).

145 AMS radiocarbon measurements that had been published earlier for selected  
146 sites of the LGC (Wohlfarth *et al.* 1998; Wohlfarth & Possnert 2000) are here used to  
147 verify the internal consistency of the new composite varve chronology (Table 1). To  
148 provide the most reliable <sup>14</sup>C-based chronology, we selected only those <sup>14</sup>C  
149 measurements that had been made on terrestrial plant macrofossil remains and we

150 disregarded dates that were associated with unidentified and reworked plant material  
151 or had analytical errors of >250 years (Wohlfarth *et al.* 1998; Wohlfarth & Possnert  
152 2000).

153       Based on Bayesian wiggle-match modelling using OxCal4.2 (Bronk Ramsey  
154 2010), these <sup>14</sup>C dates were used to find the most likely possible placement of the LGC  
155 on the IntCal13 radiocarbon calibration curve (Reimer *et al.* 2013). Outlying dates  
156 were detected by the software applying the 'Outlier Analysis' and discarded until a  
157 satisfactory and coherent age model was generated as defined by a high model  
158 agreement with values higher than a threshold of 60% (Bronk Ramsey 2009).

159

#### 160 *New cores: fieldwork, dating and elemental analyses*

161 A new sediment succession from Lake Gummetorpasjön, which was previously  
162 investigated by Wohlfarth *et al.* (1998), was cored in March 2015 (Fig. 1), with the  
163 purpose of performing geochemical analysis. Parallel sediment cores were collected  
164 using a 1-m long Russian corer with diameters of 10 and 7.5 cm, obtaining 50 cm  
165 overlapping sections.

166       Correlation to the previously established LGC chronology (Wohlfarth *et al.* 1998)  
167 was carried out employing three distinct colour and varve thickness changes that were  
168 identified by Wohlfarth *et al.* (1998). The marker layers, which occur 115 and 108  
169 varve years apart from each other, are present in the majority of the varve diagrams  
170 that compose the LGC, including Gummetorpajön (see discussion below). This allowed  
171 the new XRF profiles to be placed unequivocally within the existing chronology.

172       The new Gummetorpasjön sediment cores were scanned at the Department of  
173 Geological Sciences at Stockholm University using an ITRAX XRF Core Scanner from

174 Cox Analytical System (Gothenburg, Sweden) to detect chemical changes and signals  
175 relating to summer and winter layers. Radiographic images were generated using a  
176 Mo tube set at 55 kV and 50 mA with a step size of 200  $\mu\text{m}$  and a dwell time of 400  
177 ms. XRF data were acquired using a Mo tube set at 30 kV and 50 mA with a step size  
178 of 200  $\mu\text{m}$  and a dwell time of 30 s. Based on XRF counting statistics of the new  
179 Gummetorpasjön clay-varve record, reliable data were obtained for 21 elements with  
180 signals well above the instrumental noise threshold making it unnecessary to  
181 normalize the peak area data to the scattering. Relative changes in peak areas of  
182 elemental data were therefore used to construct ratio profiles from selected  
183 elements, i.e. Zr, Rb, Fe and Ca. Elemental XRF core scanning profiles were used as  
184 indicators of changes in sediment transfer rates and grain size mediated by local ice-  
185 mass turnover within the fjord system.

186

## 187 **Results and discussion**

### 188 *Reconstruction of the new Lateglacial varve chronology*

189 To anchor the LGC to the chronology of Gropviken, which contains the Vedde Ash, we  
190 approached the alignment systematically (see below), initially adopting Kristiansson's  
191 (1986) original time scale.

192 The first step taken for correlating the Gropviken varve thickness diagram and  
193 each one of the diagrams composing the LGC was to search for statistically significant  
194 cross-correlations between the successions, though this proved unsuccessful due to  
195 substantial differences in varve thicknesses.

196 We therefore introduced an additional alignment step by bridging Gropviken's  
197 chronology and the LGC using the Sandfjärden floating varve chronology from the

198 northern sector of Östergötland (Fig. 1C). The cross-correlation of varve thickness  
199 diagrams from Gropviken and Sandfjärden provided a statistically significant match ( $r$   
200 = 0.61, signal-to-noise ratio  $z = 7.7$ ,  $p = 0.99$ ) that enabled us to extend the varve  
201 chronology to the northern sector of Östergötland (Fig. 3).

202 In a next step we linked the Sandfjärden chronology to the LGC. However, cross-  
203 correlations alone could not directly link the two chronologies together. The  
204 chronologies were therefore aligned via identification of three common markers, i.e.  
205 two colour changes at local varve years 2060 and 2169, and a characteristic thick varve  
206 horizon at local varve year 2060 (Fig. 3). This technique (e.g. Palmer *et al.* 2010)  
207 provided satisfactory fits between the successions.

208 To provide an independent test of the alignment between the LGC and  
209 Gropviken's chronology, we employed an independent  $^{14}\text{C}$  dating method (Fig. 4). The  
210 LGC is supported by AMS radiocarbon measurements (Wohlfarth *et al.* 1998;  
211 Wohlfarth & Possnert 2000), whereas the Vedde Ash has been precisely radiocarbon  
212 dated in lake sediment records from western Norway (Lohne *et al.* 2013). The LGC was  
213 anchored to the IntCal13 radiocarbon calibration curve using a Bayesian wiggle-  
214 matching model based on eight radiocarbon dates. Using the calibrated age of the  
215 Vedde Ash and the most likely placement of the LGC on the IntCal13 time scale,  
216 respectively, we were able to calculate the offset between the chronology of  
217 Gropviken and the LGC, and compare the results with the offset previously obtained  
218 from the alignment approach. The offsets resulting from the two methods,  
219 respectively, strongly agree with each other (-1353 years using the alignment versus -  
220 1359 using wiggle-matching; Fig. 4), which indicates that the relative placement  
221 between the northern and southern chronologies is coherent and reliable.

222

223 *Age error evaluation of the Lateglacial varve chronology*

224 The excellent correlation among the 55 varve diagrams that compose the original LGC  
225 suggests no or minimal counting errors and laterally continuous varve accumulation  
226 over this sector of Småland/Östergötland (Wohlfarth *et al.* 1998). An example of such  
227 region-wide chronological consistency is demonstrated by the precision of varve  
228 counts in relation to the interval spanning the three marker horizons utilized to link  
229 the original LGC to Sandfjärden's chronology (<1% difference).

230 The independent <sup>14</sup>C dating approach described in section above provides a  
231 means to verify the chronological accuracy over a large interval of the LGC,  
232 demonstrating that contributions to uncertainty from undetected systematic errors in  
233 the varve layer identification process is minimal (Fig. 4). This is also substantiated by  
234 the similarity between the inferred varve age and the unmodelled <sup>14</sup>C-calibrated curve  
235 (Fig. 4). Moreover, the biostratigraphic boundary of the AL-YD transition, which has  
236 been identified in the pollen stratigraphy from Gummetorpasjön (Björck 1999),  
237 provides an additional chronostratigraphic constraint that confirms the internal  
238 consistency of the LGC. Indeed, even considering the low-resolution pollen sampling  
239 (Björck 1999), the estimated <sup>14</sup>C-calibrated age of this regionally isochronous marker  
240 in the varve stratigraphy falls within the 1 $\sigma$  range of the AL-YD pollen zone boundary  
241 observed in some of the most robustly constrained radiocarbon-dated regional  
242 records (Muschitiello & Wohlfarth 2015).

243 We are confident that an overall uncertainty (entailing precision and accuracy)  
244 of  $\pm 0.5\%$  ( $2\sigma$ ) is an over-conservative estimate for the unified chronology. This is based  
245 on, *i*) the general lack of disturbed or suspicious intervals and the good preservation

246 of the varves in all the LGC profiles (Wohlfarth *et al.* 1998), *ii*) the evenly high  
247 correlation among numerous adjacent and distal sites (Wohlfarth *et al.* 1998), and *iii*)  
248 the internal chronological consistency determined via independent dating  
249 approaches. This is realistic given that the error that accompanies most varve  
250 chronologies with well-developed and undisturbed successions displaying little  
251 variations between alternate counts does not exceed  $\pm 1\%$  (Zolitschka *et al.* 2015).

252

### 253 *Synchronization to Greenland Ice-Core Chronology 2005 and varve stratigraphy*

254 Our new LGC extends over  $1257 \pm 3$  varve years ( $1\sigma$ ) and covers the interval from the  
255 regional late AL pollen zone to the regional late YD pollen zone. The chronology is  
256 based on 57 varve-thickness diagrams, which were compiled to form one unified  
257 record of mean varve thickness (Fig. 5). The supporting  $^{14}\text{C}$ -based age model enables  
258 us to secure the new LGC on the IntCal13 time scale. Critically, we are also now able  
259 to synchronize the LGC record with the Greenland Ice-Core Chronology 2005  
260 (Rasmussen *et al.* 2006; after converting the b2k age [before the year 2000] into BP  
261 [before 1950 AD], hereafter GICC05 years BP) via the Vedde Ash time marker (Fig. 5).  
262 This allows us, for the first time, to directly compare the dynamics of the FIS to the  
263 Greenland ice-core event stratigraphy.

264         Although there are numerous distinct events with exceptionally thick varves,  
265 Wohlfarth *et al.* (1998) identified only three major events in their varve chronology,  
266 that are recurrent in the majority of the varve diagrams. The Events, numbered 1, 2  
267 and 3 (Wohlfarth *et al.* 1998), are characterised by distinct colour changes of the clay  
268 varves and based on the correlation to the ice core time scale occurred at 12 847, 12  
269 739 and 12 624 GICC05 years BP, within one varve year. All the events exhibit a marked

270 drop in varve thickness that lasts for a few decades. The colour change and the drop  
271 in varve thickness make Event 1, 2 and 3 different from all the other anomalous varve  
272 layers that can be observed in the new LGC.

273 Events 2 and 3, which are both preceded by an exceptionally thick varve, have  
274 been attributed to drainages of ice-dammed lakes located west of the BIL (Wohlfarth  
275 *et al.* 1998). These events are present in all varve diagrams except for Skedevi, Råfstad  
276 and Kråkedal (sites 17, 20 and 21 in Fig. 1). As such, large areas above the highest  
277 shoreline remained covered by stagnant ice and continued to contribute sediment  
278 material to the BIL as the ice sheet retreated (Lundqvist & Wohlfarth 2001). However,  
279 it remains unclear why a decrease in varve thickness accompanies all of the events.

280 Event 1 in particular, which can be observed in all the varve diagrams covering this  
281 interval (Figs. 1, 2), presents the most pronounced decrease in varve thickness of the  
282 entire chronology, but is not preceded by a thick varve (Fig. 5). This suggests that the  
283 causes of Event 1, which can be traced for more than 25 km eastwards (from  
284 Gummetorpasjön to Tynn – Wohlfarth *et al.* 1998), are potentially not just a mere  
285 response to a release of high amounts of sediment material into the BIL. Moreover,  
286 based on a previously published ice-rafted debris (IRD) record (Wohlfarth *et al.* 1998)  
287 that accompanies the LGC (Fig. 5), it is evident that, unlike Events 2 and 3, Event 1 is  
288 the only one associated with a long-term interruption (~130 varve years) in IRD  
289 deposition.

290 We note that, after synchronizing the varve record to the Greenland time scale,  
291 Event 1 coincides with the transition from Greenland Interstadial 1 to Greenland  
292 Stadial 1 (GS-1), which is defined in NGRIP ice cores as an abrupt shift in  $\delta$ -excess that  
293 took place within 2-3 years (Steffensen *et al.* 2008). The onset of GS-1 is dated to 12

294 846±69 GICC05 years BP considering 1σ age uncertainty in the GICC05 (i.e. half of the  
295 total maximum counting error – MCE; Rasmussen *et al.* 2006) and Event 1 is dated to  
296 12 847±2 GICC05 years BP (accounting for 1σ of the total uncertainty that  
297 accompanies the LGC). This places GS-1 and Event 1 at 725±6 years and 726±2 years,  
298 respectively, prior to the Vedde Ash in their respective records.

299 The temporal consistency of Event 1 relative to the start of GS-1 requires further  
300 attention. In the following, we focus on the varve stratigraphic boundary identified at  
301 12 847±71 GICC05 years BP by reporting and discussing the results from XRF analyses  
302 on Gummetorpasjön's succession in conjunction with output from idealised ice flow  
303 model simulations.

304

#### 305 *Geochemical evidence of depositional changes at the GI-1/GS-1 transition*

306 We use Zr/Rb and Fe/Ca ratios as proxies for grain-size distribution and composition  
307 (Fig. 6). Rb, which is common in several minerals, has generally low environmental  
308 mobility owing to strong sorption in clay minerals. Conversely, Zr is usually found in  
309 medium to coarse silts and is present in heavy minerals. In fine-grained sediments -  
310 like in our clay varves, Zr/Rb is thus an ideal proxy for grain size (Dypvik & Harris 2001).  
311 Like Rb, Fe absorbs onto clay and has relatively low mobility, whereas Ca can easily be  
312 found in plagioclase and calcite in the sand and silt fraction (e.g. Johnson *et al.* 2013).  
313 Thus, Fe/Ca can be used here as an additional indicator for grain size.

314 The XRF data profiles entirely resolve seasonal varves associated with summer  
315 and winter accumulation, with summer laminae generally characterised by larger  
316 grain sizes as compared to winter laminae (Fig. 6). The XRF stratigraphies consistently  
317 show a decrease in grain size 18-19 varve years before Event 1 at 12 847 GICC05 years

318 BP (Fig. 6). At 12 847 GICC05 years BP the ratio values abruptly shift indicating a  
319 change towards coarser grain sizes. The shift takes place within one varve year, after  
320 which the geochemical parameters indicate that depositional conditions directly enter  
321 into a new stable state for a period that lasted 57-58 varve years (Fig. 6).

322 We infer increased sediment supply of fine sediments during the two decades  
323 preceding Event 1, followed by a marked slowdown of sediment transfer and increase  
324 in grain size at 12847 GICC05 years BP. This is coeval with a distinct drop in varve  
325 thickness and disappearance of IRD (Fig. 5). The rapid change in varve thickness and  
326 grain size suggest a potential large-scale shift in the lake circulation regime and/or  
327 changes to how sediments are supplied to the lake.

328 Stabilisation of the ice sheet's calving margin could achieve the observed  
329 changes in IRD delivery. Increased stability can be driven by glacio-isostatic rebound  
330 of the crust and commensurate reduction in the proglacial water depth (Gomez *et al.*  
331 2010), though its gradual nature cannot explain the abrupt sedimentation changes  
332 observed in the LGC records. Rather, we suggest that a rapid fall of the BIL water level,  
333 reducing calving margin buoyancy, and therefore calving, acted to abruptly decrease  
334 iceberg calving flux from the ice margin.

335 The coupling between a rapid lowering of the BIL and a general decrease in varve  
336 thickness together with interruption of IRD deposition has been suggested for the final  
337 drainage of the BIL around the YD-Preboreal transition (Andrén *et al.* 1999, 2002). We  
338 therefore argue that the evidence in the LGC and in our geochemical records  
339 associated with Event 1 represent a late AL drainage of the BIL (Björck 1995). This  
340 would be caused by a recession of the southern margin of the FIS beyond the lake

341 outlet. In the following, we explore the implications of this hypothesis by means of  
342 simulations from a simple ice flow/calving model.

343

#### 344 *Ice-sheet response to Baltic Ice Lake drainage*

345 A series of experiments simulating a highly idealised glacier calving margin were  
346 undertaken using a well-established one-dimensional flow-line numerical model (Nick  
347 *et al.* 2010) and applying a simple floatation based calving law (Vieli *et al.* 2001). These  
348 were conducted to investigate changes in calving rate and terminus position following  
349 a drop in lake level for a flat-bedded ice sheet. These experiments do not seek to  
350 directly simulate the ice draining into the BIL, but rather illustrate the potential  
351 dynamic response of an ice sheet that experiences a drop in its proglacial lake level.  
352 The specifics of the model are discussed in detail elsewhere (e.g. Nick *et al.* 2010), with  
353 relevant input parameters shown in Table 2.

354 The model is used to investigate calving and terminus response with respect to  
355 three variables: basal roughness, initial bed depth, and size of lake-level drop. Three  
356 basal roughness scenarios were tested, chosen to represent a smooth, medium and  
357 rough sliding scenarios, with values defined within the range of those used for  
358 contemporary Greenland modelling studies (e.g. Nick *et al.* 2013; Lea *et al.* 2014a, b).  
359 Three initial bed elevations were also chosen, equivalent to the mean, 25<sup>th</sup> and 75<sup>th</sup>  
360 percentile values of a transect spanning an estimated pre-YD ice margin, isostatically  
361 depressed according to the Ice5G model (Peltier 2004). Finally, three different lake-  
362 level drops were simulated (10, 20 and 30 m), based on current estimates of the  
363 magnitude of the hypothesized pre-YD BIL drainage (Björck 1995; Bennike & Jensen  
364 2013).

365 Results of highly idealised numerical model experiments investigating calving  
366 and terminus behaviour are shown in Fig. 7. These demonstrate that in all cases a drop  
367 in lake level would cause both a reduction in calving compared to the pre-drainage  
368 iceberg flux and an advance of the ice-calving terminus. However, the magnitude of  
369 these changes, ranging from 10% to 45%, is highly dependent on the initial lake depth  
370 and size of the lake drop. While changes in calving are broadly unaffected by the basal  
371 conditions of the ice stream, Fig. 7 also shows that rougher bed conditions limit how  
372 far the glacier calving margin can advance following a lake level drop (though it should  
373 be emphasised that these should not be equated to estimates of actual advance  
374 distances of FIS following lake drainage).

375 The results provide evidence that the proportional reduction in calving rates will  
376 have been greatest in shallow areas of the BIL. Larger drops in lake level result in  
377 greater proportional decreases in calving flux, as is consistent with the floatation  
378 calving law employed in the model. However, these larger drops would also increase  
379 the range of calving response between shallow and deeper areas of the BIL  
380 terminating sectors of FIS.

381 Model results suggest that the BIL terminating sectors of the FIS will have  
382 experienced a decrease in calving flux due to decreased buoyancy (and hence  
383 stabilisation) of the ice margin. Although calving rates will have responded almost  
384 instantaneously to a drop in lake level, this is likely to only impact IRD frequency (as  
385 identified) rather than the deposition of finer grained sediments on a lake-wide scale.  
386 By itself, this can only partially explain the observed drop in IRD frequency, though it  
387 is worth noting that a thinner calving margin would also produce smaller, and  
388 therefore less long-lived icebergs. Faster melting icebergs would therefore decrease

389 the probability of IRD deposition in ice distal/sheltered parts of the post-drainage BIL.  
390 A further consideration is that changes in lake circulation resulting from the drop in  
391 BIL may have caused debris-laden icebergs to be diverted elsewhere from the coring  
392 sites.

393 The presence of thinner varves following the drainage suggests that reworking  
394 of material from newly exposed areas of the former lake bed did not result in  
395 significant sediment supply into the lake basin. We therefore hypothesise that the  
396 shift in observed sedimentation rates resulted from a rapid change in the delivery rate  
397 of subglacially derived material to the lake. However, further investigation regarding  
398 the major sediment sources for the varves would be required for this to be fully  
399 substantiated.

400

#### 401 *The first drainage of the Baltic Ice Lake*

402 During the latter part of the AL, rapid deglaciation of the southern FIS margin near Mt.  
403 Billingen - in the south-central Swedish low-land area (Fig. 1B) – is thought to have  
404 generated a spillway system that connected the BIL to the sea in the west (e.g. Björck  
405 & Möller 1987; Björck 1995; Lundqvist & Wohlfarth 2001). A rapid retreat of the FIS  
406 west of the outlet resulted in a 5-10 m lowering of the BIL (Björck 1995) also referred  
407 to as the first drainage of the BIL.

408 Although this drainage hypothesis has long been debated, new reconstructions  
409 support the occurrence of a late AL connection between the BIL and the North Atlantic  
410 (Swärd *et al.* 2015) and a significant drop of the BIL water level at this time (Bennike  
411 & Jensen 2013). Shore displacement curves from Hunneberg, west of Mt. Billingen,  
412 provide a detailed framework for the timing of the deglaciation near the outlet and

413 the freshwater connection to the sea (e.g. Björck & Digerfeldt 1982a, b). The published  
414 radiocarbon dates associated with the shoreline reconstructions have recently been  
415 re-calibrated and combined using a Bayesian framework (Muschitiello *et al.* in press).  
416 The radiocarbon dates indicate lake isolations from the sea near 11 000 <sup>14</sup>C years BP  
417 (~11000 ± 100 cal. years BP), a result of the deglaciation north of Mt. Billingen  
418 (Björck & Digerfeldt 1982a, b). Therefore, the dates provide a chronological estimate  
419 of the opening of the outlet at Mt. Billingen.

420 The combined age probability of the radiocarbon dates associated with lake  
421 isolations has been compared to the age estimate of Event 1 derived from the  
422 radiocarbon-based age model that underpins the LGC (Fig. 8). The two independent  
423 age estimates, based on wiggle-matching and on radiocarbon calibration, are  
424 remarkably similar (12867±66 cal. years BP for the opening of the outlet at Mt.  
425 Billingen versus 12876±22 cal. years BP for Event 1). The good chronological  
426 correspondence supports our hypothesis of late AL drainage of the BIL synchronous  
427 with the start of GS-1 in the Greenland ice core chronology. Furthermore, the  
428 observed offset of 30±22 years (1σ) between the GICC05 and the IntCal13 time scales  
429 at the transition into GS-1 (Fig. 8) compares well with an offset of 40±30 years (1σ)  
430 estimated with other independent methods of time-scale synchronization (Muscheler  
431 *et al.* 2014).

432 We suggest that Event 1 can provide a precise chronological tie point that can  
433 facilitate regional correlations for future varve reconstructions. In addition, this  
434 stratigraphic marker - and more broadly any direct evidence of the first drainage of  
435 the BIL - can potentially be used as an isochronous horizon to link records from the

436 Baltic Sea, southern Sweden and the eastern sector of the North Sea downstream of  
437 the drainage route.

438

#### 439 *Palaeoclimatic implications*

440 The abrupt shift in *d*-excess values that marks the onset of GS-1 in the NGRIP ice cores  
441 (Steffensen *et al.* 2008) can be ascribed to a large southward shift of the marine  
442 moisture source for Greenland precipitation (Pfahl & Sodemann 2014) driven by a  
443 southward displacement of the North Atlantic westerly winds (Muschitiello *et al.* in  
444 press). It has been hypothesised that such an abrupt southward diversion of the  
445 westerly winds could have been triggered by a comparably abrupt westward  
446 expansion of sea ice in the Nordic Seas (Muschitiello *et al.* in press). However, the  
447 driving forces behind this putative swift growth of regional sea ice are still not entirely  
448 discerned.

449         A catastrophic drainage of freshwater from the BIL can provide a plausible  
450 explanation for a westward migration of sea ice in the Nordic Seas, and especially for  
451 its abruptness, thereby providing a physical mechanism and timing for the start of GS-  
452 1. We hypothesize that a powerful surge of Baltic-sourced freshwater routed north  
453 along the coast of the Norwegian Sea could have increased sea-ice production and  
454 moved, to some extent, sea ice off the shelf area towards the open ocean or  
455 recirculated ice in the Nordic Seas. Thus, the excess sea ice was displaced westwards  
456 beyond the limits expected from local climatological growth conditions and ultimately  
457 exported to the subpolar North Atlantic. This phenomenon could have induced the  
458 atmospheric circulation to cross thresholds beyond which the seasonal distribution of  
459 sea ice in the Nordic Seas became significantly altered, instigating a widespread

460 expansion of sea ice in the North Atlantic. Nonetheless, this explanation remains  
461 speculative until more detailed climate modelling studies surrounding the  
462 atmosphere-ocean response to Fennoscandian meltwater outlets can be undertaken.

463

#### 464 **Conclusions**

465 In this study we have reevaluated and extended a Swedish Lateglacial varve chronology,  
466 which now forms a continuous 1257-year long record spanning the period from the  
467 regional late AL to the late YD pollen zone. The chronology has been secured to the  
468 GICC05 and IntCal13 absolute time scales. Correlation to the Greenland ice-core  
469 framework allows us, for the first time, to compare the melting history of the FIS with  
470 ice-core climate events.

471 By using geochemical analyses and ice-flow modelling simulations, we suggest  
472 that in the late AL a major drop of the BIL water level associated with the first drainage  
473 of the BIL occurred. The drainage took place synchronously with the start of GS-1 and  
474 specifically  $726 \pm 2$  years prior to the deposition of the Vedde Ash as compared to  
475  $725 \pm 6$  years observed in ice-core records. The drainage event would provide a  
476 plausible physical explanation for the timing and sign of hydroclimatic shifts observed  
477 in the Greenland records, while the related stratigraphic marker can serve as an  
478 important chronological tie-point for future regional correlation of proxy records.

479 We hope that this study will inspire future water-hosing and eddy-resolving  
480 ocean model simulations that can help to shed light on the forcing mechanisms behind  
481 the rapid climate changes that took place at the inception of Greenland Stadial 1 in  
482 the North Atlantic region.

483

484 *Acknowledgements.* - We are kindly grateful to P. Saarikoski for assistance during  
485 fieldwork and M. Kylander for help with XRF core scanning. We are also grateful to  
486 M.D. Johnson and an anonymous reviewer for helpful comments on an earlier version  
487 of the manuscript. The contribution of JL was supported by FORMAS grant 214-2013-  
488 1600 (PI: Nina Kirchner, Stockholm University). This work is a contribution to the  
489 INTIMATE project.

490

#### 491 **References**

492 Andrén, T., Björck, J. & Johnsen, S. 1999: Correlation of Swedish glacial varves with the  
493 Greenland (GRIP) oxygen isotope record. *Journal of Quaternary Science* 14, 361–  
494 371.

495 Andrén, T., Lindeberg, G. & Andrén, E. 2002: Evidence of the final drainage of the Baltic  
496 Ice Lake and the brackish phase of the Yoldia Sea in glacial varves from the Baltic  
497 Sea. *Boreas* 31, 226–238.

498 Anjar, J., Larsen, N.K., Håkansson, L., Möller, P., Linge, H., Fabel, D. & Xu, S. 2014: A  
499 <sup>10</sup>Be-based reconstruction of the last deglaciation in southern Sweden. *Boreas*  
500 43, 132-148.

501 Bennike, O. & Jensen, J.B. 2013: A Baltic Ice Lake lowstand of latest Allerød age in the  
502 Arkona Basin, southern Baltic Sea. *Geological Survey of Denmark and Greenland*  
503 *Bulletin* 28, 17–20.

504 Björck, S. 1979: Late Weichselian stratigraphy of Blekinge, SE Sweden, and water level  
505 changes in the Baltic Ice Lake. *LUNDQUA Thesis* 7, 248 pp.

506 Björck, J. 1999. The Allerød-Younger Dryas pollen zone boundary in an 800-year varve  
507 chronology from southeastern Sweden. *GFF* 121, 287–292.

508 Björck, S., 1995: A review of the history of the Baltic Sea, 13.0-8.0 ka BP. *Quaternary*  
509 *International* 27, 19–40.

510 Björck, S. Digerfeldt, G., 1982a: New <sup>14</sup>C dates from Hunneberg supporting the revised  
511 deglaciation chronology of the Middle Swedish end moraine zone. *GFF* 103, 395–  
512 404.

513 Björck, S. Digerfeldt, G., 1982b: Late Weichselian shore displacement at Hunneberg,  
514 southern Sweden, indicating complex uplift. *GFF* 104, 131–155.

- 515 Björck, S. & Digerfeldt, G. 1984: Climatic changes at Pleistocene/Holocene boundary  
516 in the Middle Swedish End Moraine Zone, mainly inferred from stratigraphic  
517 indications. In Mörner, N.A., Karlén, W. (eds): *Climatic Changes on a Yearly to*  
518 *Millennial Basis*. Reidel Publishing Co., Dordrecht, pp37-56.  
519
- 520 Björck, S. & Möller, P. 1987: Late Weichselian environmental history in southeastern  
521 Sweden during the deglaciation of the Scandinavian ice sheet. *Quaternary*  
522 *Research* 28, 1–37.
- 523 Björck, S., Cato, I., Brunnberg, L. & Strömberg, B. 1992: The clay-varve based Swedish  
524 Time Scale and its relation to the Late Weichselian radiocarbon chronology. *In*  
525 *The Last Deglaciation: Absolute and Radiocarbon Chronologies*, 25–44. Springer,  
526 Berlin.
- 527 Bronk Ramsey, C. 2009: Bayesian analysis of radiocarbon dates. *Radiocarbon* 51, 337–  
528 360.
- 529 Bronk Ramsey, C. 2010: OxCal Program, v. 4.1.7, Radiocarbon accelerator unit,  
530 University of Oxford, UK.
- 531 Brunnberg, L. 1995: Clay-varve chronology and deglaciation during the Younger Dryas  
532 and Preboreal in the easternmost part of the Middle Swedish Ice Marginal Zone.  
533 *Quaternaria Series A* 2, 1-95.
- 534 Cato, I. 1985: The definitive connection of the Swedish geochronological time scale  
535 with the present, and the new date of the zero year in Döviken, northern Sweden.  
536 *Boreas* 14, 117–122.
- 537 Cato, I. 1987: On the definitive connection of the Swedish Time Scale with the present.  
538 *Sveriges Geologiska Undersökning Ca* 68. 55 pp.
- 539 Cato, I. 1998: Ragnar Lidén's Postglacial Varve Chronology from the Ångermanälvan  
540 Valley, Northern Sweden. *Sveriges Geologiska Undersökning Ca* 88. 82 pp.
- 541 Cuffey, K.M. & Paterson, W.S.B. 2010: *The physics of glaciers*. 704 pp. Butterworth-  
542 Heinemann, Oxford.
- 543 De Geer, G. 1912: Geochronology of the last 12,000 years. *Proceedings of the*  
544 *International Geological Congress 1910*, 241-253.
- 545 De Geer, G. 1940. Geochronologia Suecica Principles. *Kungliga Svenska*  
546 *Vetenskapsakademiens Handlingar, Tredje Serien Band* 18, No. 6, 367 pp.
- 547 Dypvik, H. & Harris, N.B. 2001: Geochemical facies analysis of fine-grained siliciclastics  
548 using Th/U, Zr/Rb and (Zr+ Rb)/Sr ratios. *Chemical Geology* 181, 131–146.
- 549 Gomez, N., Mitrovica, J.X., Huybers, P. & Clark, P.U. 2010: Sea level as a stabilizing  
550 factor for marine-ice-sheet grounding lines. *Nature Geoscience* 3, 850–853.

- 551 Goslar, T., Wohlfarth, B., Björck, S., Possnert, G. & Björck, J. 1999: Variations of  
552 atmospheric  $^{14}\text{C}$  concentrations over the Allerød-Younger Dryas transition.  
553 *Climate Dynamics* 15, 29–42.
- 554 Holmquist, B. & Wohlfarth, B. 1998: An evaluation of the Late Weichselian Swedish  
555 varve chronology based on cross-correlation analysis. *GFF* 120, 35–46.
- 556 Johnsen, T.F., Alexanderson, H., Fabel, D. & Freeman, S.P.H.T. 2009: New  $^{10}\text{Be}$   
557 cosmogenic ages from the Vimmerby moraine confirm the timing of  
558 Scandinavian Ice Sheet deglaciation in southern Sweden. *Geografiska Annaler*  
559 91A, 113-120.
- 560 Johnson, M.D., Kylander, M.E., Casserstedt, L., Wiborgh, H. & Björck, S. 2013:  
561 Glaciomarine varved clay in central Sweden before and after the Baltic Ice Lake  
562 drainage: a further clue to the drainage events at Mt Billingen. *GFF* 135, 293-  
563 307.
- 564 Kristiansson, J. 1986: The ice recession on the southeastern part of Sweden.  
565 Stockholm, *University of Stockholm, Department of Quaternary Research, Report*  
566 7, 133 pp.
- 567 Lea, J. M., Mair, D. W., Nick, F. M., Rea, B. R., Weidick, A., Kjaer, K. H., Morlighem, M.,  
568 Van As, D. & Schofield, J. E. 2014: Terminus-driven retreat of a major southwest  
569 Greenland tidewater glacier. *Journal of Glaciology*, 60, 333-344.
- 570 Lea, J.M., Mair, D.W.F., Nick, F.M., Rea, B.R., As, D.V., Morlighem, M., Nienow, P. &  
571 Weidick, A. 2014: Fluctuations of a Greenlandic tidewater glacier driven by  
572 changes in atmospheric forcing: observations and modelling of Kangiata  
573 Nunaata Sermia, 1859–present. *The Cryosphere*, 8, 2031-2045.
- 574 Lohne, O.S., Mangerud, J. & Birks, H.H. 2013: Precise  $^{14}\text{C}$  ages of the Vedde and  
575 Saksunarvatn ashes and the Younger Dryas boundaries from western Norway and  
576 their comparison with the Greenland Ice Core (GICC05) chronology. *Journal of*  
577 *Quaternary Science* 28, 490–500.
- 578 Lundqvist, J. 1987: Glaciodynamics of the Younger Dryas marginal zone in Scandinavia.  
579 Implications of a revised glaciation model. *Geografiska Annaler* 69A, 305-319.  
580
- 581 Lundqvist, J. & Wohlfarth, B. 2001: Timing and east–west correlation of south Swedish  
582 ice marginal lines during the Late Weichselian. *Quaternary Science Reviews* 20,  
583 1127–1148.
- 584 Macleod, A., Brunberg, L., Wastegård, S., Hang, T. & Matthews, I.P. 2014: Lateglacial  
585 cryptotephra detected within clay varves in Östergötland, south-east Sweden.  
586 *Journal of Quaternary Science* 29, 605–609.

- 587 Muscheler, R., Adolphi, F. & Knudsen, M.F. 2014: Assessing the differences between  
588 the IntCal and Greenland ice-core time scales for the last 14,000 years via the  
589 common cosmogenic radionuclide variations. *Quaternary Science Reviews* 106,  
590 81-87.
- 591 Muschitiello, F. & Wohlfarth, B. 2015: Time-transgressive environmental shifts across  
592 Northern Europe at the onset of the Younger Dryas. *Quaternary Science Reviews*  
593 109, 49–56.
- 594 Muschitiello, F., Pausata, F.S.R., Watson, J.E., Smittenberg, R.H., Salih, A.A.M., Brooks,  
595 S.J., Whitehouse, N.J. Karlatou-Charalampopoulou, A. & Wohlfarth, B. in press:  
596 Fennoscandian freshwater control on Greenland hydroclimate shifts at the  
597 onset of the Younger Dryas. *Nature Communications*.
- 598 Nick, F.M., Van der Veen, C.J., Vieli, A. & Benn, D.I. 2010: A physically based calving  
599 model applied to marine outlet glaciers and implications for the glacier  
600 dynamics. *Journal of Glaciology*, 56, 781-794.
- 601 Nick, F.M., Vieli, A., Andersen, M.L., Joughin, I., Payne, A., Edwards, T.L. & van de Wal,  
602 R.S. 2013: Future sea-level rise from Greenland/'s main outlet glaciers in a  
603 warming climate. *Nature*, 497, 235-238.
- 604 Palmer, A.P., Rose, J., Lowe, J.J. & MacLeod, A. 2010: Annually resolved events of  
605 Younger Dryas glaciation in Lochaber (Glen Roy and Glen Spean), Western  
606 Scottish Highlands. *Journal of Quaternary Science*, 25, 581-596.
- 607 Peltier, W.R. 2004: Global glacial isostasy and the surface of the ice-age Earth: the ICE-  
608 5G (VM2) model and GRACE. *Annual Reviews of Earth and Planetary Sciences* 32,  
609 111–149.
- 610 Pfahl, S. & Sodemann, H. 2014: What controls deuterium excess in global  
611 precipitation? *Climate of the Past* 10, 771–781.
- 612 Rasmussen, S.O., Andersen, K.K., Svensson, A.M., Steffensen, J.P., Vinther, B.M.,  
613 Clausen, H.B., Siggaard-Andersen, M.L., Johnsen, S.J., Larsen, L.B., Dahl-Jensen,  
614 D., Bigler, M., Röthlisberger, R., Fischer, H., Goto-Azuma, K., Hansson, M.E. &  
615 Ruth, U. 2006: A new Greenland ice core chronology for the last glacial  
616 termination. *Journal of Geophysical Research: Atmospheres* 111, D061202.
- 617 Reimer, P.J., Bard, E., Bayliss, A., Beck, J.W., Blackwell, P.G., Bronk Ramsey, C., Buck,  
618 C.E., Cheng, H., Edwards, R.L. & Friedrich, M. 2013: IntCal13 and Marine13  
619 radiocarbon age calibration curves 0-50,000 years cal BP. *Radiocarbon* 55,1869-  
620 1887.
- 621 Steffensen, J.P., Andersen, K.K., Bigler, M., Clausen, H.B., Dahl-Jensen, D., Fischer, H.,  
622 Goto-Azuma, K., Hansson, M., Johnsen, S.J., Jouzel, J., Masson-Delmotte, V.,  
623 Popp, T., Rasmussen, S.O., Rothlisberger, R., Ruth, U., Stauffer, B., Siggaard-  
624 Andersen, M.-L., Sveinbjrnsdottir, A.E., Svensson, A. & White, J.W.C. 2008: High-

- 625 Resolution Greenland Ice Core Data Show Abrupt Climate Change Happens in  
626 Few Years. *Science* 321, 680–684.
- 627 Swärd, H., O’Regan, M., Ampel, L., Ananyev, R., Chernykh, D., Flodén, T., Greenwood,  
628 S.L., Kylander, M.E., Mörth, C.M., Preto, P. & Jakobsson, M. 2015: Regional  
629 deglaciation and postglacial lake development as reflected in a 74 m sedimentary  
630 record from Lake Vättern, southern Sweden. *GFF*, 1-19.
- 631 Vieli, A., Funk, M. & Blatter, H. 2001: Flow dynamics of tidewater glaciers: a numerical  
632 modelling approach. *Journal of Glaciology*, 47, 595-606.
- 633 Wohlfarth, B. 1996: The chronology of the last termination: a review of radiocarbon-  
634 dated, high-resolution terrestrial stratigraphies. *Quaternary Science Reviews* 15,  
635 267–284.
- 636 Wohlfarth, B. & Possnert, G. 2000: AMS radiocarbon measurements from the Swedish  
637 varved clays. *Radiocarbon* 42, 323–334.
- 638 Wohlfarth, B., Björck, S., Possnert, G., Lemdahl, G., Brunnberg, L., Ising, J., Olsson, S.  
639 & Svensson, N.-O. 1993: AMS dating Swedish varved clays of the last  
640 glacial/interglacial transition and the potential/difficulties of calibrating Late  
641 Weichselian “absolute” chronologies. *Boreas* 22, 113–128.
- 642 Wohlfarth, B., Björck, S., Holmqvist, B., Lemdahl, G. & Ising, J. 1994: Ice recession and  
643 depositional environment in the Blekinge archipelago of the Baltic Ice Lake. *GFF*  
644 116, 3–12.
- 645 Wohlfarth, B., Björck, S. & Possnert, G. 1995: The Swedish time scale; a potential  
646 calibration tool for the radiocarbon time scale during the late Weichselian.  
647 *Radiocarbon* 37, 347–359.
- 648 Wohlfarth, B., Björck, S., Cato, I. & Possnert, G. 1997: A new middle Holocene varve  
649 diagram from the river Ångermanälven, northern Sweden: indications for a  
650 possible error in the Holocene varve chronology. *Boreas* 26, 347–353.
- 651 Wohlfarth, B., Björck, S., Possnert, G. & Holmquist, A.N.D.B. 1998: 800-year long,  
652 radiocarbon-dated varve chronology from south-eastern Sweden. *Boreas* 27,  
653 243-258.
- 654 Zolitschka, B., Francus, P., Ojala, A.E.K. & Schimmelmann, A. 2015: Varves in lake  
655 sediments – a review. *Quaternary Science Reviews* 117, 1–41.

656

657 **Figure and Table captions**

658 **Figure 1.** A. Locations of southern Sweden and NGRIP ice cores. B, C. Location of the  
659 sites used to construct the new Lateglacial varve chronology in southern Sweden.  
660 Black circles refer to sites studied by Wohlfarth *et al.* (1995). Red circles refer to sites  
661 studied by Kristiansson (1986). Blue numbers indicate the sites where the depositional  
662 Event 1 (Wohlfarth *et al.* 1998) was identified (see text for details). Note that Event 1  
663 can be observed in all the varve diagrams that cover the related time interval. Ice  
664 marginal positions are based on Lundqvist & Wohlfarth (2001) and visual  
665 interpretation of moraine positions from the LiDAR-based topography. The  
666 southernmost ice marginal line refers to the Younger Dryas ice limit (YD). The  
667 northernmost ice marginal line refers to the ice limit shortly before the last drainage  
668 of the Baltic Ice Lake. Highest shoreline data from Geological Survey of Sweden on a  
669 colour scale graded according to present-day elevation (highest lake position was  
670 time-transgressive: yellow to red). 1= Bjärka-Säby; 2= Skaggebo; 3= Nåtvin; 4=  
671 Vårdnäs; 5= Järnlunden/Stensvassa; 6= Limmern; 7= Storsjön; 8, 9= Mjölsjön; 10=  
672 Järnlunden/Sonebo; 11= Bjärsjön; 12, 13, 14= Glottern; 15= Eknäs; 16= Rimforsa; 17=  
673 Skedevi; 18= Ytterbo; 19= Räfstad; 20= Äfsinge; 21= Åsunden/Krågedal; 22= Vigerstad;  
674 23= Hägerstad; 24= Rävantorpasjön; 25= Lillsjön; 26= Drättinge; 27= Boda; 28=  
675 Årteryd; 29= Utdala; 30= Stjärnevik; 31= Tynn/Tyllinge; 32= Tynn/Draboviken; 33=  
676 Nedre Emmaren; 34= Bjuggö; 35= Kärra; 36= Lövdalen; 37= Gumhem; 38= Långebro;  
677 39, 40, 41= Hargsjön ; 42= Hargsjön 1; 43= Kisa; 44, 45= Adlerskogsjön; 46, 47=  
678 Gummetorpasjön ; 48= Kristineberg; 49= Greby; 50= Åby; 51= Väsby; 52= Dråpetorp;  
679 53= Brunebo; 54= Järpekullen; 55= Kåreda. The location of Gropviken and Sandfjärden  
680 is also shown (green circles). LiDAR topography © Lantmäteriet.

681

682 **Figure 2.** Length of the varve-thickness diagrams used to construct the chronology  
683 presented in Wohlfarth *et al.* (1998) and displayed on the local varve time scale  
684 proposed by Kristiansson (1986). The chronology is based on diagrams studied by  
685 Kristiansson (1986) and Wohlfarth *et al.* (1995), which were visually and statistically  
686 cross-correlated with each other (Holmqvist & Wohlfarth 1998). Numbers refer to the  
687 original coding scheme used by Holmqvist & Wohlfarth (1998). The three major  
688 depositional events identified by Wohlfarth *et al.* (1998) are also shown at the bottom.  
689 The events are characterised by distinct colour changes of the clay varves and a  
690 marked drop in varve thickness that last for a few decades (see text for details).

691

692 **Figure 3.** Varve-width and stratigraphic alignment of the varve records forming the  
693 new composite Lateglacial varve chronology from Småland/Östergötland presented  
694 on the local varve time scale (Kristiansson 1986). The two northernmost successions  
695 of Gropviken and Sandfjärden were first cross-correlated with each other. Prior to  
696 cross-correlation time series were detrended applying a 16<sup>th</sup> degree Fourier  
697 transform, filtered using a 3-year moving average and removing the first 10 bottom  
698 varves, and normalized by their standard deviation. The correlation coefficient ( $r$ ) and  
699 statistics (signal-to-noise ratio  $z$  and  $p$ -value) between the individual records are given  
700 in the graph. Sandfjärden's chronology was correlated to the 806-year long master  
701 chronology (Wohlfarth *et al.* 1998) via common stratigraphic markers (two marked  
702 colour changes and an exceptionally thick varve layer). The master chronology  
703 presented here was filtered by removing the first 10 bottom varves of each varve  
704 diagram.

705

706 **Figure 4.** Top panel: Wiggle-matching age model of the Lateglacial varve chronology  
707 (LGC) and verification of its placement relative to the chronology of Gropviken  
708 containing the Vedde Ash time marker. The age model of the LGC is based on  
709 radiocarbon dates from selected terrestrial plant macrofossils previously published in  
710 Wohlfarth *et al.* (1998) (blue crosses; Table 1). A radiocarbon-based calendar age for  
711 the Vedde Ash in Gropviken (red cross) was assigned using precise estimates from  
712 Lake Kråkenes in Western Norway (Lohne *et al.* 2013). The most likely position of each  
713 radiocarbon estimate on the modelled IntCal13 calibration curve (grey; Reimer *et al.*  
714 2013) is shown. In the upper-left panel is presented the comparison of the estimated  
715 offsets between the LGC and Gropviken using cross-correlation and radiocarbon-  
716 based methods, respectively (see text for details). The goodness of the placement of  
717 the LGC relative to Gropviken is further confirmed by the position of the Allerød-  
718 Younger Dryas pollen-defined boundary on the master chronology, which is consistent  
719 with previously reported age estimates for this biostratigraphic event (Muschitiello &  
720 Wohlfarth 2015). The probability distribution functions of the most likely placement  
721 on the IntCal13 time scale of the LGC and the Vedde Ash, respectively, are also shown  
722 together with their 2 sigma standard error. Bottom panel: Plot showing varve-age  
723 against depth (blue dots and dashed line). The varve-age-depth relationship is  
724 compared to the calibrated  $^{14}\text{C}$  curve based on the unmodelled radiocarbon  
725 measurements listed in Table 1 (black dots). Bars indicate 2 sigma standard error  
726 associated with each measurement and the additional varve-age error related to  
727 macrofossil sampling (Wohlfarth *et al.* 1998). The varve-age scale is based on  
728 synchronization to the IntCal13 time scale using the radiocarbon-based age estimate  
729 of the Vedde Ash (red dot).

730

731 **Figure 5.** The new Lateglacial varve chronology presented as a unified record of mean  
732 varve thickness and plotted against the GICC05 time scale (after converting the b2k  
733 age into BP) and IntCal13 time scale after synchronization via the Vedde Ash isochron  
734 and wiggle-match modelling, respectively. Mean annual varve widths are displayed  
735 together with a 10-year running average (red line). The chronology is plotted with a  
736 record of ice-rafted mineral debris (blue histogram) formerly published in Wohlfarth  
737 *et al.* (1998). The vertical dashed lines indicate the interval analysed for ice-rafted  
738 debris grains. The three major depositional events identified by Wohlfarth *et al.* (1998)  
739 are also displayed. The green bar shows the timing of the regional AL-YD pollen  
740 boundary as defined in the Lateglacial varve chronology (Björck, 1999), which lags the  
741 onset of Greenland Stadial 1 by ~150 years.

742

743 **Figure 6.** XRF elemental results from new Gummetorpasjön's varve records. All data  
744 are smoothed using a 10-point running mean to facilitate visualization (black line). For  
745 reference, the XRF data are presented with the optical and radiographic  
746 stratigraphies. The stratigraphic transition referred to as Event 1 and synchronous  
747 with the start of Greenland Stadial 1 in ice-core records is highlighted by the red  
748 dashed line. The XRF elemental profiles consistently show relative changes in ratio  
749 values 18-19 varve years before Event 1 (shaded area). Note inverse axis for Zr/Rb  
750 ratios.

751

752 **Figure 7.** Results of idealised model runs showing change in calving fluxes and  
753 terminus position 10 years after an instantaneous drop in lake level is applied. These

754 are shown for three different initial lake levels, and three different potential lake level  
755 drops. These experiments were run for (A) low, (B) medium, and (C) high basal  
756 roughness scenarios.

757

758 **Figure 8.** Calendar age of Event 1 in the new Lateglacial varve chronology relative to  
759 the GICC05 and IntCal13 time scale and compared with estimated age of the start of  
760 Greenland Stadial 1 in Greenland ice cores. The age of Event 1 is also compared with  
761 the combined probability of a number of calibrated radiocarbon dates constraining  
762 the timing of the first drainage of the Baltic Ice Lake and presented in Muschitiello *et*  
763 *al.* (in press). The calibrated radiocarbon dates refer to lake isolations from the sea,  
764 which indicate timing of deglaciation of the outlet system west of Mount Billingen in  
765 southern Sweden, near 11 000 <sup>14</sup>C years BP (Björck and Digerfledt 1982a, b). Two dates  
766 refer to isolation owing to concomitant lowering of the Baltic Ice Lake in Blekinge  
767 (Björck 1979) and one refers to the timing of the Baltic Ice Lake water-level fall as  
768 recorded in Arkona Basin, southern Baltic Sea (Bennike & Jensen 2013). All ages are  
769 here presented with their 1 sigma uncertainty and error bars. Under the assumption  
770 of synchronicity between Event 1, the first drainage of the Baltic Ice Lake and the onset  
771 of Greenland Stadial 1, the estimated offset between the GICC05 (after converting the  
772 b2k age into BP) and the IntCal13 time scales at the transition into Greenland Stadial  
773 1 is of 30±22 years (1σ).

774

775 **Table 1.** AMS <sup>14</sup>C dates from glacialacustrine varves of the Östergötland master  
776 chronology. All dates are based on selected terrestrial plant remains and used to  
777 construct the Bayesian wiggle-matching age model presented in this study.

778

779 **Table 2.** Input parameters used in the ice flow/calving model experiments.

780

Table Error! No sequence specified.

Sample ID	Site	Local Varve Years	<sup>14</sup> C age (year)	<sup>14</sup> C error (1 sigma)	Used in the age model
Ua-11233	Nedre Emmaren	2221±52	10 740	240	No
Ua-10181	Gummetorpasjön	2199±32	11 450	240	No
Ua-11234	Nedre Emmaren	2146±23	10 885	250	Yes
Ua-3131	Tynn	2125±35	10 890	120	Yes
Ua-10182	Gummetorpasjön	2123±30	11 470	130	No
Ua-10183	Gummetorpasjön	2090±18	11 030	120	Yes
Ua-4358	Hargsjön	2055±50	10 980	100	Yes
Ua-10184	Gummetorpasjön	2044±16	10 970	90	Yes
Ua-2753	Hargsjön	2010±45	10 480	150	No
Ua-10185	Gummetorpasjön	2009±16	11 230	100	No
Ua-4493	Adlerskogssjön	2003±59	10 830	165	Yes
Ua-4359	Hargsjön	1973±31	10 610	110	Yes
Ua-10186	Gummetorpasjön	1968±25	11 040	110	No
Ua-10187	Gummetorpasjön	1938±4	10 420	220	Yes
Ua-4496	Glottarn	1856±50	10 585	465	No

781

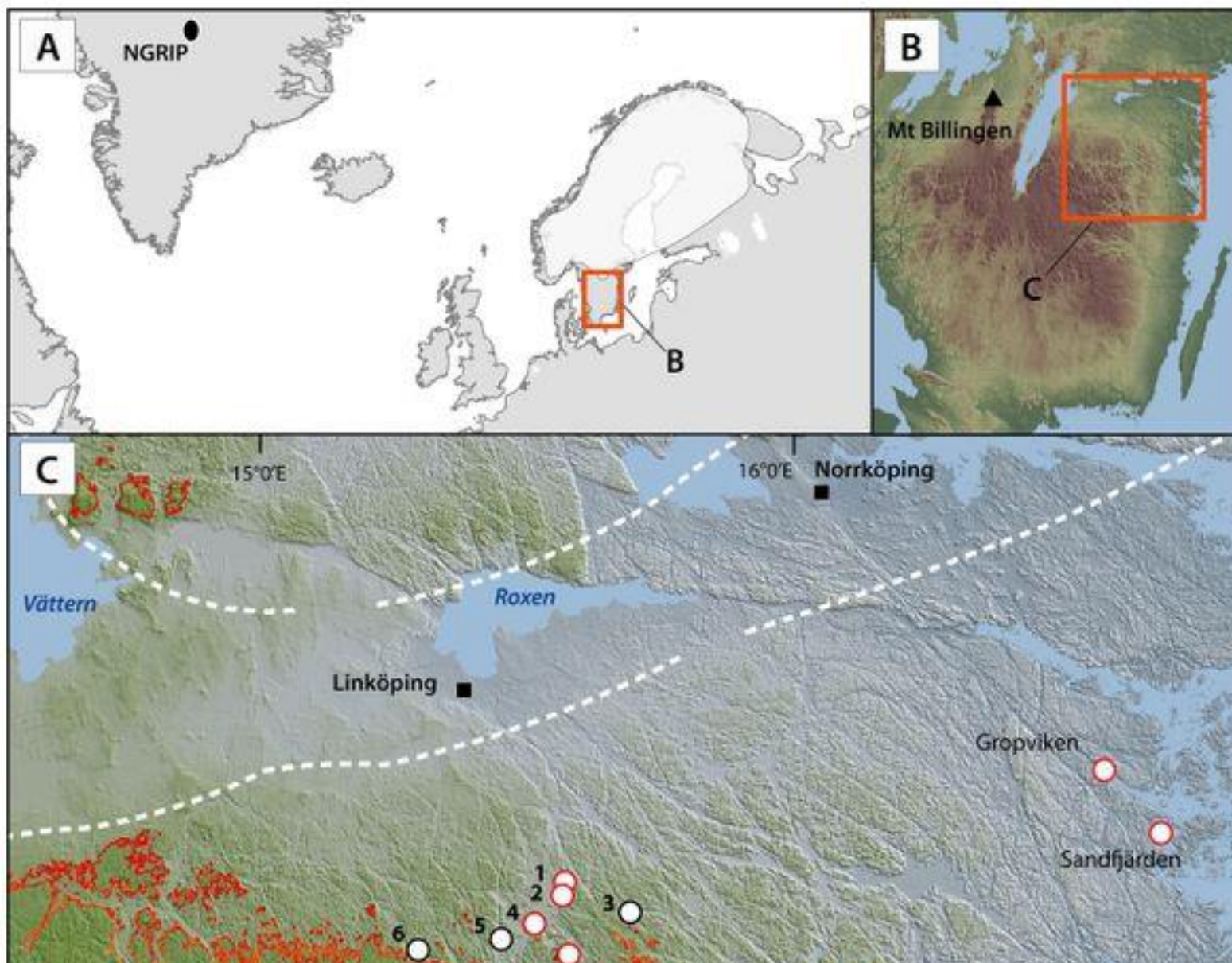
782

783

Table 2

Parameter/Constant	Value
Ice density – $\rho_i$	900 kg m <sup>-3</sup>
Meltwater density – $\rho_w$	1000 kg m <sup>-3</sup>
Proglacial water body density – $\rho_p$	1000 kg m <sup>-3</sup>
Gravitational acceleration - $g$	9.8 m s <sup>-2</sup>
Friction exponent - $m$	3
Excess floatation fraction - $q$	0.09
Glen's flow law exponent - $n$	3
Glen's flow law coefficient - $A$	2.93 x 10 <sup>-17</sup> Pa <sup>-3</sup> a <sup>-1</sup> Corresponding to -5 °C (Cuffey & Paterson, 2010)
Initial grid size	~250 m
Time step	0.005 a

784  
785



Fig

